

# Oxidative Addition Reactions of $[\text{Rh}^{\text{I}}(\text{Br})(\text{Tpy}^*)]$ ( $\text{Tpy}^* = 4'-(4\text{-tert-Butylphenyl})-2,2':6',2''\text{-terpyridine}$ ) with Alkyl Bromides

Boke C. de Pater, Eric J. Zijp, Hans-Werner Frühauf,\* Jan M. Ernsting, Cornelis J. Elsevier, and Kees Vrieze

*Coordination and Organometal Chemistry, Institute of Molecular Chemistry, University of Amsterdam, Nieuwe Achtergracht 166, 1018 WV Amsterdam, The Netherlands*

Peter H. M. Budzelaar and Anton W. Gal

*Department of Inorganic Chemistry, University of Nijmegen, Toernooiveld 1, 6525 ED Nijmegen, The Netherlands*

Received July 17, 2003

Oxidative addition reactions with the highly nucleophilic complex  $[\text{Rh}^{\text{I}}(\text{Cl})(4'-(4\text{-tert-butylphenyl})-2,2':6',2''\text{-terpyridine})]$  (**1**) and alkyl halides containing chlorine and bromine atoms gave mixtures of uncharacterized products. In contrast to this, oxidative addition reactions with the complex  $[\text{Rh}^{\text{I}}(\text{Br})(4'-(4\text{-tert-butylphenyl})-2,2':6',2''\text{-terpyridine})]$  (**2**) and various alkyl bromides, containing (mainly terminal) carbon–bromine bonds, gave clean single products in almost quantitative yield. The corresponding air-stable yellow Rh(III)–terpyridine complexes are, in contrast to the parent Rh(I)–terpyridine complex, soluble in various organic solvents. Consequently, these products have been further characterized by means of  $^1\text{H}$ ,  $^{13}\text{C}$ ,  $^{15}\text{N}$ ,  $^{103}\text{Rh}$  and 2D NMR techniques. NMR techniques were also used to determine the geometry of the studied Rh(III)–terpyridine complexes, which were found to be octahedral with the alkyl moiety axially positioned with respect to the Rh–terpyridine plane (except for complexes **3** and **4**). The oxidative addition reaction of complex **2** with 1-bromodecane in ethanol was monitored by UV/vis spectrometry. The recorded electronic absorption spectrum of this reaction showed two distinct isosbestic points in the visible region. It is most likely that first the carbon–bromine bond of 1-bromodecane is activated by the Rh metal followed by the arrangement of the alkyl moiety in an axial position. Unfortunately, on the basis of our findings, no single mechanism for this oxidative addition reaction can be suggested.

## Introduction

Oxidative addition reactions are a general synthetic method for the formation of carbon–metal  $\sigma$ -bonds.<sup>1</sup> Most reported syntheses of carbon–metal  $\sigma$ -bonds involve the reaction of alkyl iodides and bromides with compounds of gold,<sup>2</sup> platinum,<sup>3–5</sup> palladium,<sup>6</sup> iridium,<sup>7–12</sup>

and rhodium.<sup>13–18</sup> In particular, the oxidative addition reaction of MeI to carbonylrhodium complexes has been studied in great mechanistic detail, since it is the key step in the catalyzed carbonylation of methanol on an industrial scale.<sup>19–22</sup> Furthermore, rhodium–alkyl complexes are considered to be key intermediates in major industrially important catalytic processes such as hydrogenation and hydroformylation.<sup>23</sup>

\* To whom correspondence should be addressed. E-mail: hwf@science.uva.nl. Fax: +31-20-525 6456.

- (1) Stille, J. K.; Lau, K. S. Y. *Acc. Chem. Res.* **1977**, *10*, 434.
- (2) Fackler, J. P., Jr. *Polyhedron* **1997**, *16*, 1.
- (3) Baar, C. R.; Jenkins, H. A.; Vittal, J. J.; Yap, G. P. A.; Puddephatt, J. R. *Organometallics* **1998**, *17*, 2805.
- (4) Scott, J. D.; Puddephatt, J. R. *Organometallics* **1986**, *5*, 2522.
- (5) Ling, S. S. M.; Jobe, I. R.; Manojlovic-Muir, L.; Muir, K. W.; Puddephatt, J. R. *Organometallics* **1985**, *4*, 1198.
- (6) Balch, A. L.; Hunt, C. T.; Lee, C.-L.; Olmstead, M. M.; Farr, J. P. *J. Am. Chem. Soc.* **1981**, *103*, 3764.
- (7) Bushnell, G. W.; Fjeldsted, D. O. K.; Stobart, S. R.; Wang, J. *Organometallics* **1996**, *15*, 3785.
- (8) Pinillos, M. T.; Elduque, A.; Martín, E.; Navarro, N.; Lahoz, F. J.; López, J. A.; Oro, L. A. *Inorg. Chem.* **1995**, *34*, 111.
- (9) Asseid, F.; Browning, J.; Dixon, K. R.; Meanwell, N. J. *Organometallics* **1994**, *13*, 760.
- (10) Kolel-Veetil, M. K.; Rheingold, A. L.; Ahmend, K. J. *Organometallics* **1993**, *12*, 3439.
- (11) El Amame, M.; Maisonnat, A.; Dahan, F.; Poilblanc, R. *New J. Chem.* **1988**, *12*, 661.
- (12) Labinger, J. A.; Osborn, J. A. *Inorg. Chem.* **1980**, *19*, 3230.

- (13) Tejel, C.; Ciriano, M. A.; Edwards, A. J.; Lahoz, F. J.; Oro, L. A. *Organometallics* **1997**, *16*, 45.
- (14) Elduque, A.; Garcés, Y.; Oro, L. A.; Pinillos, M. T.; Tiripicchio, A.; Ugozzoli, F. *J. Chem. Soc., Dalton Trans.* **1996**, 2155.
- (15) Ciriano, M. A.; Pérez-Torrente, J.; Lahoz, F. J.; Oro, L. A. *J. Organomet. Chem.* **1994**, *482*, 53.
- (16) He, X.-D.; Maisonnat, A.; Dahan, F.; Poilblanc, R. *Organometallics* **1991**, *10*, 2443.
- (17) Venter, J. A.; Leipoldt, J. G.; Van Eldik, R. *Inorg. Chem.* **1991**, *30*, 2207.
- (18) Schenck, T. G.; Milne, C. R. C.; Sawyer, J. F.; Bosnich, B. *Inorg. Chem.* **1985**, *24*, 2338.
- (19) Forster, D. *Adv. Organomet. Chem.* **1979**, *17*, 255.
- (20) Forster, D.; Singleton, T. C. *J. Mol. Catal.* **1982**, *17*, 299.
- (21) Parshall, G. W.; Ittel, S. D. *Homogeneous Catalysis*, 2nd ed.; Wiley-Interscience: New York, 1992.
- (22) Ellis, P. R.; Pearson, J. M.; Haynes, A.; Adams, H.; Bailey, N. A.; Maitlis, P. M. *Organometallics* **1994**, *13*, 3215.
- (23) Dickson, R. S. *Homogeneous Catalysis with Compounds of Rhodium and Iridium*; D. Reidel: Dordrecht, The Netherlands, 1985.

Oxidative addition reactions of carbon–halogen bonds to transition-metal complexes are also applied in a number of other industrially important catalytic processes. Examples of these are the cross-coupling and carbonylation reactions of aryl halides for e.g. the syntheses of drugs and fragrances.<sup>24,25</sup> More recently, since compounds containing carbon–halogen bonds have been used in large amounts over the last century (agriculture, industry, home products, etc.), their potential danger for the environment has created considerable concern.<sup>26–30</sup> Therefore, it is very important to develop catalysts to transform compounds with carbon–halogen bonds into harmless molecules in order to neutralize the potential danger of organohalide pollutants. This can be achieved by either stoichiometric reactions<sup>31</sup> or biological processes,<sup>32,33</sup> which can be facilitated by catalysts<sup>34–36</sup> and enzymes (respectively).

On the basis of the many mechanistic studies,<sup>23,37–43</sup> using e.g. square-planar d<sup>8</sup> metal complexes,<sup>44,45</sup> several mechanisms have been proposed for the oxidative addition reaction of alkyl halides. The most common mechanisms noted in the literature are the S<sub>N</sub>2<sup>1,46,47</sup> and the concerted cis-addition<sup>17</sup> mechanisms and mechanisms involving free alkyl radical intermediates.<sup>38,48</sup> Recent theoretical studies of the oxidative addition reaction of MeX (X = Cl, I) to Pd, Rh, and Ir complexes suggest that the preferred pathway is S<sub>N</sub>2.<sup>49,50</sup> In addition, kinetic studies on the oxidative addition reac-

tion of many carbon–halogen bonds to a Rh(I) complex suggest a general S<sub>N</sub>2-like mechanism.<sup>51</sup>

The reactivity of metal-containing complexes toward oxidative addition reactions with carbon–halogen bonds is highly dependent on the electron density of the metal center.<sup>52–66</sup> For example, breaking carbon–chloride  $\sigma$ -bonds is only possible when very electron rich centers are used.<sup>64,67–72</sup> Therefore, in comparison to alkyl iodides and bromides, oxidative addition reactions of the less reactive alkyl chlorides are scarcer.<sup>73</sup> The design of complexes with electron-rich metal centers is based on the use of strongly electron-donating ligands. Terdentate nitrogen-containing ligands have proven to be very successful in this respect. Itoh et al. studied the in situ oxidative addition of alkyl chlorides with rhodium complexes using the [Rh(Cl)(cyclooctene)<sub>2</sub>] precursor and the 2,6-bis(4,4-dimethylloxazolin-2-yl)pyridine (dm-pybox) ligand.<sup>69</sup> Furthermore, Haarman et al.<sup>74</sup> successfully showed that the very electron rich complexes [Rh<sup>I</sup>(Cl)(2,6-(C(R<sup>1</sup>)=NR<sup>2</sup>)<sub>2</sub>C<sub>5</sub>H<sub>3</sub>N)]<sup>75</sup> with terdentate pyridine–diimine ligands are highly reactive toward various substrates containing carbon–chloride  $\sigma$ -bonds. It was found that chloroform, dichloromethane, benzyl chloride, and  $\alpha,\alpha$ -dichlorotoluene readily undergo oxidative addition reactions, even at low temperatures (–96 °C).<sup>74</sup> The terdentate pyridine–diimine ligand is not only increasing the reactivity of the Rh center but, due to its chelating capability, also stabilizes the oxidative

(24) Beller, M.; Cornils, B.; Frohning, C. D.; Kohlpainter, C. W. *J. Mol. Catal. A: Chem.* **1995**, *104*, 17.

(25) Cornils, B.; Herrmann, W. A. *Applied Homogeneous Catalysis with Organometallic Compounds (A Comprehensive Handbook in Two Volumes)*; VCH: Weinheim, Germany, 1996.

(26) McElroy, M. E.; Salawitch, R. J.; Wofsy, S. C.; Logan, J. A. *Nature (London)* **1986**, *321*, 755.

(27) Crutzen, P. J. *Angew. Chem., Int. Ed. Engl.* **1996**, *35*, 1758.

(28) Molina, M. J. *Angew. Chem., Int. Ed. Engl.* **1996**, *35*, 1778.

(29) Rowland, F. S. *Angew. Chem., Int. Ed. Engl.* **1996**, *35*, 1787.

(30) Saunders, G. C. *Angew. Chem., Int. Ed. Engl.* **1996**, *35*, 2615.

(31) Rondon, D.; He, X.-D.; Chaudret, B. *J. Organomet. Chem.* **1992**, *433*, C18.

(32) Gottschalk, G.; Knackmuss, H. J. *Angew. Chem., Int. Ed. Engl.* **1993**, *32*, 1398.

(33) Müller, R.; Lingens, F. *Angew. Chem., Int. Ed. Engl.* **1986**, *25*, 779.

(34) Ferrughelli, D. T.; Horváth, I. T. *J. Chem. Soc., Chem. Commun.* **1992**, 806.

(35) Grushin, V. V.; Alper, H. *Organometallics* **1991**, *10*, 1620.

(36) Labat, G.; Seris, J. L.; Meunier, B. *Angew. Chem., Int. Ed. Engl.* **1990**, *29*, 1471.

(37) Halpern, J. *Acc. Chem. Res.* **1970**, *3*, 386.

(38) Labinger, J. A.; Osborn, J. A.; Coville, N. J. *Inorg. Chem.* **1980**, *19*, 3236.

(39) Collman, J. P.; Hegedus, L. S.; Norton, J. R.; Finke, R. G. *Principles and Applications of Organotransition Metal Chemistry*; University Science Books: Mill Valley, CA, 1987; Vol. 2.

(40) Collman, J. P.; Roper, W. R. *Adv. Organomet. Chem.* **1968**, *7*, 53.

(41) Atwood, J. D. In *Inorganic and Organometallic Reaction Mechanisms*; Brooks/Cole: Monterey, CA, 1985.

(42) Vaska, L. *Acc. Chem. Res.* **1968**, *1*, 335.

(43) Lukehart, C. M. In *Fundamental Transition Metal Organometallic Chemistry*; Brooks/Cole: Monterey, CA, 1985.

(44) Ferguson, G.; Monaghan, P. K.; Parvez, M.; Puddephatt, J. R. *Organometallics* **1985**, *4*, 1669.

(45) Hill, R. H.; Puddephatt, J. R. *J. Am. Chem. Soc.* **1985**, *107*, 1218.

(46) Oro, L. A.; Sola, E.; Lopéz, J. A.; Torres, F.; Elduque, A.; Lahoz, F. J. *Inorg. Chem. Commun.* **1998**, *1*, 64.

(47) Von Zelewsky, A.; Suckling, A. P.; Stoeckli-Evans, H. *Inorg. Chem.* **1993**, *32*, 4585.

(48) Hall, T. L.; Lappert, M. F.; Lednor, P. W. *J. Chem. Soc., Dalton Trans.* **1980**, 1448.

(49) Bickelhaupt, F. M.; Ziegler, T.; Schleyer, P. v. R. *Organometallics* **1995**, *14*, 2288.

(50) Griffin, T. R.; Cook, D. B.; Haynes, A.; Pearson, J. M.; Monti, D.; Morris, G. E. *J. Am. Chem. Soc.* **1996**, *118*, 3029.

(51) Collman, J. P.; Brauman, J. I.; Madonik, A. M. *Organometallics* **1986**, *5*, 310.

(52) Paul, W.; Werner, H. *Chem. Ber.* **1985**, *118*, 3032.

(53) Werner, H.; Hofmann, L.; Feser, R.; Paul, W. *J. Organomet. Chem.* **1985**, *281*, 317.

(54) Werner, H.; Paul, W.; Feser, R.; Zolk, R.; Thometzek, P. *Chem. Ber.* **1985**, *118*, 261.

(55) El Amame, M.; Maisonnat, A.; Dahan, F.; Pince, R.; Poilblanc, R. *Organometallics* **1985**, *4*, 773.

(56) Moss, J. R.; Pelling, S. J. *J. Organomet. Chem.* **1982**, *236*, 221.

(57) Kermodé, N. J.; Lappert, M. F.; Skelton, B. W.; White, A. H.; Holton, J. *J. Chem. Soc., Chem. Commun.* **1981**, 698.

(58) Gash, R. C.; Cole-Hamilton, D. J.; Whyman, R.; Barnes, J. C.; Simpson, M. C. *J. Chem. Soc., Dalton Trans.* **1994**, 1963.

(59) Burns, E. G.; Chu, S. S. C.; De Meester, P.; Lattman, M. *Organometallics* **1986**, *5*, 2383.

(60) Olson, W. L.; Nagaki, D. A.; Dahl, L. F. *Organometallics* **1986**, *5*, 630.

(61) Scherer, O. J.; Jungmann, H. *J. Organomet. Chem.* **1981**, *208*, 153.

(62) Ball, G. E.; Cullen, W. R.; Fryzuk, M. D.; James, B. R.; Rettig, S. J. *Organometallics* **1991**, *10*, 3767.

(63) Collman, J. P.; Murphy, D. W.; Dolcetti, G. J. *J. Am. Chem. Soc.* **1973**, *95*, 2687.

(64) Ciriano, M. A.; Tena, M. A.; Oro, L. A. *J. Chem. Soc., Dalton Trans.* **1992**, 2123.

(65) Fennis, P. J.; Budzelaar, P. H. M.; Frijns, J. H. G.; Orpen, A. G. *J. Organomet. Chem.* **1990**, *393*, 287.

(66) Marder, T. B.; Fultz, W. C.; Calabrese, J. C.; Harlow, R. L.; Milstein, D. *J. Chem. Soc., Chem. Commun.* **1987**, 1543.

(67) Ghilardi, C. A.; Midollini, S.; Moneti, S.; Orlandini, A.; Ramirez, J. A. *J. Chem. Soc., Chem. Commun.* **1989**, 304.

(68) Winter, C. A.; Gladysz, J. A. *J. Organomet. Chem.* **1988**, *354*, C33.

(69) Nishiyama, H.; Horiata, M.; Wakamatsu, T.; Itoh, K. *Organometallics* **1991**, *10*, 2706.

(70) Chen, Q.; Marzilli, L. G.; Bresciani Pahor, N.; Randaccio, L.; Zangrando, E. *Inorg. Chim. Acta* **1988**, *144*, 241.

(71) Ogino, H.; Shomi, M.; Abe, Y.; Shimura, M.; Shimoi, M. *Inorg. Chem.* **1987**, *26*, 2543.

(72) Huser, M.; Youinou, M.-T.; Osborn, J. A. *Angew. Chem., Int. Ed. Engl.* **1989**, *28*, 1386–1388.

(73) Tejel, C.; Ciriano, M. A.; Edwards, A. J.; Lahoz, F. J.; Oro, L. A. *Organometallics* **2000**, *19*, 4968–4976.

(74) Haarman, H. F.; Ernsting, J. M.; Kranenburg, M.; Kooijman, H.; Veldman, N.; Spek, A. L.; Van Leeuwen, P. W. N. M.; Vrieze, K. *Organometallics* **1997**, *16*, 887.

(75) Haarman, H. F.; Bregman, F. R.; Ernsting, J. M.; Veldman, N.; Spek, A. L.; Vrieze, K. *Organometallics* **1997**, *16*, 54.

addition product, facilitating its full characterization. Finally, crystallographic studies strongly indicated that the Rh–C  $\sigma$ -bond, formed after the oxidative addition reaction with  $CHCl_3$  or  $CH_2Cl_2$  and  $[RhCl(2,6-(C(R^1)=NR^2)_2C_5H_3N)]$ , has a metal–carbene ( $Rh=C^+Cl^-$ ) character.<sup>74,76–79</sup>

These interesting features displayed by the square-planar complexes  $[Rh^I(Cl)(2,6-(C(R^1)=NR^2)_2C_5H_3N)]$  toward oxidative addition reactions with alkyl halides prompted us to study similar rhodium complexes of terpyridine ligands. Unlike the work of Haarman et al.,<sup>74</sup> the oxidative addition reactions with  $[Rh^I(X)(Tpy^*)]$  ( $X = Cl, Br$  for complexes **1** and **2**, respectively) and chlorocarbons gave mixtures of unidentified products. Only oxidative addition reactions with  $[Rh^I(Br)(Tpy^*)]$  (**2**) and mainly primary alkyl bromides afforded the formation of clean single products (**4–24**). Here we report the successful oxidative-addition reactions between complex **2** and numerous reagents containing primarily terminal C–Br bonds.

## Experimental Section

**General Considerations.** The 4'-(4-*tert*-butylphenyl)-2,2':6',2''-terpyridine ( $Tpy^*$ ) ligand was synthesized according to literature procedures,<sup>80,81</sup> while its purification was executed differently: i.e., column chromatography with silica gel using a 6:1:4 eluent mixture of toluene, diethyl ether, and hexane.<sup>82</sup> The syntheses of the complexes **1–24** were performed under an inert atmosphere of purified argon, using standard Schlenk techniques. If not stated otherwise, for the syntheses of these complexes, 0.028 g of  $[RhBr(COD)]_2$  (0.048 mmol, COD = 1,5-cyclooctadiene) and 0.035 g of  $Tpy^*$  (0.096 mmol) were used. The yield of the products **1–23** was practically quantitative, while the yield of **24** was ca. 70%. Solvents were dried and purified by standard procedures. The bromine reagents, used for the synthesis of complexes **3–24**, were purchased from Aldrich.<sup>83</sup> The  $^1H$  and  $^{13}C$  NMR spectra were recorded at 294 K with Bruker AMX 300, Bruker DRX 300, Varian Mercury 300, and Varian Inova 500 spectrometers. All  $^1H$  and  $^{13}C$  NMR signal assignments of complexes **3a,b** and **4–24** are based on NMR studies for the signal assignments of complex **10** also using mathematical simulations and 2D NMR techniques such as COSY (H,H) and HMQC (H,C) measurements. The  $^{15}N$  NMR spectra were recorded using the PFG HMQC sequence<sup>84–87</sup>

(76) Van Leeuwen, P. W. N. M.; Roobeek, C. F.; Huis, R. J. *Organomet. Chem.* **1977**, *142*, 233 and 243.

(77) McCrindle, R.; Arsenaull, G. J.; Gupta, A.; Hampden-Smith, M. J.; Rice, R. E.; McAlees, A. J. *J. Chem. Soc., Dalton Trans.* **1991**, 949.

(78) McCrindle, R.; Ferguson, G.; McAlees, A. J.; Arsenaull, G. J.; Gupta, A.; Jennings, M. C. *Organometallics* **1995**, *14*, 2741.

(79) Gandelman, M.; Rytchinski, B.; Ashkenazi, N.; Gauvin, R. M.; Milstein, D. *J. Am. Chem. Soc.* **2001**, *123*, 5372–5373.

(80) Spahni, W.; Calzaferri, G. *Helv. Chim. Acta* **1984**, *67*, 450–454.

(81) Constable, E. C.; Harverson, P.; Smith, D. R.; Whall, L. A. *Tetrahedron* **1994**, *50*, 7799–7806.

(82) The products to be separated dissolve, but do not elute, very well in toluene. Diethyl ether elutes all products adequately. Hexane enhances the separation of each single product. First, a greenish oil eluted from the column, followed by the  $Tpy^*$  ligand (main product). Finally, the diketone intermediate (incomplete formation of the  $Tpy^*$  ligand) was collected. The last two products are colorless (i.e. white).

(83) The bromine reagents provided by Aldrich were superior to those from Acros Chimica. Deliveries from Acros Chimica always gave mixtures of products, instead of single clean products when reagents were purchased from Aldrich.

(84) Hurs, R. E.; John, B. K. *J. Magn. Reson.* **1991**, *91*, 648.

(85) Ruiz-Cabello, J.; Vuister, G. W.; Moonen, C. T. W.; Van Gelderen, P.; Cohen, J. S.; Van Zijl, P. C. M. *J. Magn. Reson.* **1992**, *100*, 281–303.

(86) Wilker, W.; Leibfritz, D.; Kerssebaum, R.; Bermel, W. *J. Magn. Reson.* **1993**, *31*, 287–292.

in a Bruker DRX 300 spectrometer equipped with a 5 mm triple-resonance inverse probe with  $z$  gradient, operating at 30.42 MHz  $^{15}N$  frequency, and a second 300 W X decoupler giving a  $90^\circ$   $^{15}N$  pulse of 10  $\mu s$ . Spectra were recorded without decoupling  $^{15}N$  in  $f_2$ . The spectral width in  $f_1$  was 500 ppm, and 32 increments were used. Three values for  $J\{^1H, ^{15}N\}$  (2.5, 5, 10 Hz) were used to determine the  $^{15}N$  resonance; after the  $^{15}N$  resonance was found, the final experiment was done with a spectral width in  $f_1$  of 50 ppm and between 64 and 128 increments. This resulted, after linear prediction in  $f_1$ , in a resolution better than 0.2 ppm for the  $^{15}N$  resonance. Chemical shifts were referenced to external nitromethane at 0 ppm; negative chemical shifts are reported for lower frequencies. Spectra were recorded at 296 K. The  $^{103}Rh$  NMR measurements were performed as part of the characterization of the Rh(III) terpyridine complexes.  $^{103}Rh$  measurements were carried out on a Bruker DRX 300 spectrometer under temperature control at 298 K using a 5 mm triple-resonance inverse probe head ( $^1H, ^{31}P\{BB\}$ ) with a  $z$  gradient coil ( $90^\circ$   $^1H$ , 7.2 ms;  $90^\circ$   $^{103}Rh$ , 19.5 ms) using the PFG HMQC sequence.<sup>84–86,88</sup> The acquisition time was 30–90 min for the final experiment. The spectral width was 10 ppm for  $^1H$ . In the first measurement, the spectral width for  $^{103}Rh$  was 9000 ppm, which was covered by 128 t1 increments; 16 dummy scans were used. To exclude folding and improve resolution, a second and sometimes third measurement with modified  $n_0(Rh)$  values and smaller spectral widths were carried out; the final experiment was 500 ppm in  $f_1$  and using 256 increments. The digital resolution of  $\delta(^{103}Rh)$  was at least 3.7 Hz  $pt^{-1}$ . After a linear prediction in the  $f_1$  direction, a  $512 \times 512$  matrix was transformed, applying a sine bell weighing function. The  $^{103}Rh$  spectra are obtained in  $f_1$  and the  $^1H$  spectra in  $f_2$ . The absolute  $^{103}Rh$  ppm values are referenced to  $\Xi = 3.16$  MHz. Signals at higher frequencies are taken as positive. Fast atom bombardment (FAB<sup>+</sup>) mass spectrometry was carried out using a JEOL JMS SX/SX103a four-sector mass spectrometer, coupled to a JEOL MS-7000 data system. The samples were loaded in a matrix phase (glycerol) on a stainless steel probe and bombarded with xenon atoms with an energy of 3 keV. During the high-resolution FAB-MS measurements a resolving power of 5000 (10% valley definition) was used. CsI and glycerol were used to calibrate the mass spectrometer. Elemental analyses were carried out by H. Kolbe Mikroanalytisches Laboratorium (Mülheim an der Ruhr, Germany) and Analytische Laboratorien GmbH (Lindlar, Germany). For unknown reasons, the Rh(I) complexes with the  $Tpy^*$  ligand, i.e., **1** and **2**, notoriously gave unsatisfactory elemental analyses. Perhaps they are much more sensitive to air and moisture than analogous complexes without the 4'-(4-*tert*-butylphenyl) substituents on the terpyridine, a number of which we have described and characterized, including elemental analyses and X-ray structures.<sup>89</sup>

The reactants for the syntheses of the Rh(III)–terpyridine complexes are shown in Table 1.

Atom numbering of the Rh(III)–terpyridine complexes for the assignment of NMR signals is done according to Chart 1. **Syntheses.  $[Rh^I(Cl)(Tpy^*)]$  (**1**).** Toluene (40 mL) was added to 0.030 g of  $[RhCl(COD)]_2$  (0.061 mmol) and 0.044 g of  $Tpy^*$  (0.12 mmol). This mixture was stirred at room temperature for about 5 min, after which a dark blue precipitate was formed. After the supernatant liquid was decanted, the solid residue was washed with pentane ( $3 \times 10$  mL). After the product was dried by removing the solvent under reduced pressure, 0.06 g of complex **1** (yield ca. 99%) was collected as a dark blue powder. FAB<sup>+</sup> MS:  $m/z$  503.07 [ $M^+$ ].

(87) Milani, B.; Marson, A.; Zangrando, E.; Mestroni, G.; Ernsting, J. M.; Elsevier, C. J. *Inorg. Chim. Acta* **2002**, *327*, 188–201.

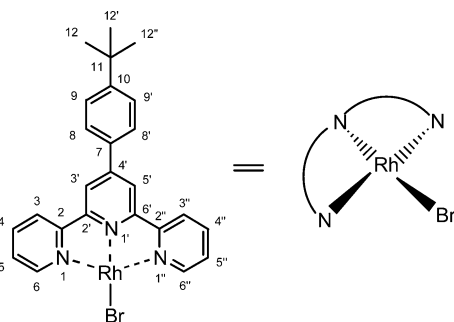
(88) Donkervoort, J. G.; Bühl, M.; Ernsting, J. M.; Elsevier, C. J. *Eur. J. Inorg. Chem.* **1988**, *27*, 7–33.

(89) de Pater, B. C.; Frühauf, H.-W.; Hartl, F.; Vrieze, K.; Budzelaar, P. H. M.; Gal, W. G.; De Gelder, R.; Baerends, E. J.; McCormack, D.; Lutz, M.; Spek, A. L. *Eur. J. Inorg. Chem.*, in press.



**Table 1. Reactants for Oxidative Addition Reactions**

reactant (complex)	
saturated	unsaturated
Br <sub>2</sub> ( <b>5</b> )	(2-bromobenzylidene)isopropylamine ( <b>3</b> , <b>4</b> )
bromomethane ( <b>6</b> )	bromoethene ( <b>14</b> )
1-bromoethane ( <b>7</b> )	3-bromopropene ( <b>15</b> )
1-bromopropane ( <b>8</b> )	3-bromo-2-methylpropene ( <b>16</b> )
1-bromobutane ( <b>9</b> )	4-bromobutene ( <b>17</b> )
1-bromopentane ( <b>10</b> )	5-bromopentene ( <b>18</b> )
1-bromohexane ( <b>11</b> )	6-bromohexene ( <b>19</b> )
1-bromooctane ( <b>12</b> )	8-bromooctene ( <b>20</b> )
1-bromodecane ( <b>13</b> )	11-bromoundecene ( <b>21</b> )
	bromobenzene ( <b>22</b> )
	benzyl bromide ( <b>23</b> )
	diphenylbromomethane ( <b>24</b> )

**Chart 1. Numbering of the Tpy\* Atoms**

**[Rh<sup>I</sup>(Br)(Tpy\*)] (**2**).** Ethanol (30 mL) was added to 0.023 g of [RhBr(COD)]<sub>2</sub> (0.039 mmol) and 0.029 g of Tpy\* (0.079 mmol). This mixture was stirred at room temperature, and after ca. 10 min a dark blue precipitate was formed. After the supernatant liquid was decanted, the remaining solid residue was washed with pentane (3 × 10 mL). After the product was dried by removing the solvent under reduced pressure, 0.043 g of complex **2** (yield ca. 99%) was collected as a dark blue powder. FAB<sup>+</sup> MS: *m/z* 547.01 [M<sup>+</sup>].

**[(2-(isopropylimino)phenyl)Rh<sup>III</sup>(X)(Tpy\*)]<sup>+</sup>Y<sup>-</sup> (**3a,b**).** Ethanol (40 mL) was added to 0.028 g of [RhCl(COD)]<sub>2</sub> (0.057 mmol) and 0.041 g of Tpy\* (0.11 mmol). This mixture was refluxed for 5 min, and **1** precipitated out of the solution. After the mixture was cooled to ca. 35 °C, >100 equiv of 2-(isopropylimino)bromobenzene was added to this mixture. When the reaction mixture was stirred for 2–3 min, a yellow suspension was formed. The product mixture was poured into pentane (150 mL). After the supernatant liquid was decanted, the remaining solid residue was washed with pentane (3 × 10 mL). After the product was dried by removing the solvent under reduced pressure, 0.078 g of a 30:70 product mixture of **3a** and **3b** (yield ca. 90%) was collected as a yellow powder (**3a**, X = Cl; **3b**, X = Br; Y = Cl, Br). With an FAB mass measurement peaks of *m/z* 649.16 and 693.11 were detected for **3a** (–Br) and **3b** (–Cl), respectively. <sup>1</sup>H NMR (300 MHz Varian Mercury 300, CD<sub>3</sub>OD, 298 K, δ): 9.11 (d, <sup>3</sup>J(Rh,H) = 3.0 Hz, 1H (19)), 9.03 (s, 2H (3',5')), 8.78 (d, 8.1 Hz, 2H (3,3')), 8.22 (2H (4,4')), 8.20 (d, 7.5 Hz, 2H (6,6')), 8.14 (d, 8.4 Hz, 2H (8,8')), 7.75 (d, 8.1 Hz, 2H (9,9')), 7.74 (1H (17)), 7.62 (t, 6.8 Hz, 2H (5,5')), 7.05 (t, 7.2 Hz, 1H (16)), 6.89 (t, 7.1 Hz, 1H (15)), 6.31 (**3a**, d, 7.8 Hz, 1H (14)), 6.23 (**3b**, d, 7.5 Hz, 1H (14)), 5.30 (**3b**, t, 6.6 Hz, 1H (20)), 5.13 (**3a**, t, 6.3 Hz, 1H (20)), 1.85 (d, 6.6 Hz, 6H (21)), 1.44 (s, 9H (*tert*-butyl)). FAB<sup>+</sup> MS: *m/z* 649.16 [(M<sub>3a</sub><sup>+</sup>) – Br], 693.11 [(M<sub>3b</sub><sup>+</sup>) – Cl].

**[(2-(isopropylimino)phenyl)Rh<sup>III</sup>(Br)(Tpy\*)]<sup>+</sup>Br<sup>-</sup> (**4**).** A solution of [RhBr(COD)]<sub>2</sub> and Tpy\* in 20 mL of ethanol was refluxed for 10 min, giving [Rh<sup>I</sup>(Br)(Tpy\*)] (**3**) as a dark blue solid. After cooling, to this mixture was added >100 equiv of 2-(isopropylimino)bromobenzene. After several minutes of stirring a yellow emulsion was formed. The product mixture

was poured into pentane (150 mL). After the supernatant liquid was decanted, the remaining solid residue was washed with pentane (3 × 10 mL). After the product was dried by removing the solvent under reduced pressure, complex **4** (yield ca. 95%) was collected as a pale yellow powder. <sup>1</sup>H NMR (500 MHz, Varian Inova 500, CD<sub>3</sub>OD, 298 K, δ): 9.11 (d, <sup>3</sup>J(Rh–N–H) = 3 Hz, 1H (19)), 9.03 (s, 2H (3',5')), 8.78 (d, 8.0 Hz, 2H (3,3')), 8.22 (t, 8.5 Hz, 2H (4,4')), 8.20 (d, 6.0 Hz, 2H (6,6')), 8.14 (d, 8.0 Hz, 2H (8,8')), 7.74 (t, 8.5 Hz, 2H (9,9')), 7.74 (d, 8.0 Hz, 1H (17)), 7.62 (t, 6.5 Hz, 2H (5,5')), 7.05 (t, 7.5 Hz, 1H (16)), 6.90 (t, 7 Hz, 1H (15)), 6.23 (8 Hz, 1H (14)), 5.29 (m, 6.5 Hz, 1H (20)), 1.85 (d, 6.5 Hz, 6H (21)), 1.44 (s, 9H (*tert*-butyl)). <sup>13</sup>C{<sup>1</sup>H} NMR (125 MHz, Varian Inova 500, CD<sub>3</sub>OD, 298 K, δ): 174.23 (C19), 165.94 (d, <sup>1</sup>J(Rh,C13) = 29.5 Hz), 157.24 (C2',C6'), 154.92 (C2,C2'), 154.42 (C10), 153.49 (C4'), 152.07 (6,6'), 145.35 (C18), 140.23 (4,4'), 133.16 (C7), 131.77 (C15), 130.75 (C17), 130.15 (C14), 128.28 (C5,C5'), 127.65 (C8,C8'), 126.61 (C9,C9'), 125.45 (C3,C3'), 125.01 (16), 121.81 (C3',C5'), 60.00 (C20), 34.70 (C11), 30.41 (C12), 22.78 (C21). <sup>103</sup>Rh NMR (3.16 MHz, 300 Bruker DRX, CD<sub>3</sub>OD, 298 K, δ): 3220.75. <sup>15</sup>N NMR (30.42 MHz, 300 Bruker DRX, CD<sub>3</sub>OD, 298 K, δ): –112.16 (N2), –140.55 (N1'), –151.92 (N1,N1'). Anal. Calcd for C<sub>35</sub>H<sub>35</sub>N<sub>4</sub>RhBr<sub>2</sub> (772.03): C, 54.28; H, 4.56; N, 7.23; Br, 20.64. Found: C, 54.15; H, 4.48; N, 7.12; Br, 20.59. FAB<sup>+</sup> MS: *m/z* 693.11 [(M<sup>+</sup>) – Br].

**[Rh<sup>III</sup>(Br)<sub>3</sub>(Tpy\*)] (**5**).** At room temperature 100 equiv of Br<sub>2</sub> was added to a deep dark blue mixture of **2** (0.079 mmol) and EtOH (20 mL). Instantaneously, a yellow emulsion was formed. The product mixture was poured into pentane (150 mL). After the supernatant liquid was decanted, the remaining solid residue was washed with pentane (3 × 10 mL). After the product was dried by removing the solvent under reduced pressure, complex **5** (yield ca. 99%) was collected as a yellow powder. <sup>1</sup>H NMR (300 MHz, 300 Bruker AMX, CD<sub>2</sub>Cl<sub>2</sub>, δ): 9.68 (d, 4.5 Hz, 2H (6,6')), 8.36 (s, 2H (3',5')), 8.28 (d, 8.4 Hz, 2H (3,3')), 8.13 (t, 7.8 Hz, 2H (4,4')), 7.79 (d, 8.7 Hz, 2H (8,8')), 7.72 (t, 8.0 Hz, 2H (5,5')), 7.68 (d, 8.7 Hz, 2H (9,9')), 1.41 (s, 9H (*tert*-butyl)). <sup>103</sup>Rh NMR (3.16 MHz, 300 Bruker DRX, CD<sub>2</sub>-Cl<sub>2</sub>, δ): 4530.13. Anal. Calcd for C<sub>25</sub>H<sub>23</sub>N<sub>3</sub>RhBr<sub>3</sub> (704.85): C, 42.41; H, 3.27; N, 5.93; Br, 33.8. Found: C, 42.36; H, 3.22; N, 5.84; Br, 33.78. FAB<sup>+</sup> MS: *m/z* 627.93 [(M<sup>+</sup>) – Br].

**[(R)Rh<sup>III</sup>(Br)<sub>2</sub>(Tpy\*)] (**6–24**).** At room temperature ca. 100 equiv of Br–R (Table 1) was added to a deep dark blue mixture of **2** (0.079 mmol) and EtOH (20 mL). After completion of the reaction a yellow solution (**10–13**, **16**, **18–21**, **23**, **24**) or emulsion (**6–9**, **14**, **15**, **17**, **22**) was formed. The product mixture was poured into pentane (150 mL). After the supernatant liquid was decanted, the remaining solid residue was washed with pentane (3 × 10 mL). After the precipitate was dried by removing the solvent under reduced pressure, the product was collected as a yellow powder (yield ca. 99% for **6–23** and ca. 70% for **24**). Reaction times, FAB mass spectral data, and elemental analyses are given in Table 2, and atom numbering is given in Table 3.

Complexes **4–24** are air-stable and soluble in various organic solvents (e.g. MeOH, EtOH, and dichloromethane). However, for the measurement of their NMR spectra (cf. Tables 4 and 5), in various cases (**5**, **7–9**, **14**, **15**, **17**, **18**, **22**) a few drops of trifluoroethanol (CF<sub>3</sub>CH<sub>2</sub>OH) were added to enhance their solubility in deuterated dichloromethane for NMR studies.

**Monitoring the Formation of Complex 13 with UV/Vis Spectroscopy.** A standard cuvette was filled with 4 mL of an ethanolic solution of complex **2** (1.23 × 10<sup>-4</sup> M) under an inert nitrogen atmosphere (glovebox). To this solution was added 5 μL of 1-bromodecane (50 equiv) for the oxidative addition reaction, which was monitored with an HP8453 diode-array spectrophotometer at 298 K. In total, 75 electronic absorption spectra were recorded with a 60 s interval between each single measurement (4500 s total measuring time). The

**Table 2. Reaction Time for Complex 2 (0.079 mmol) and Ca. 100 Equiv of Alkyl Bromides in EtOH (20 mL), FAB/Mass ( $m/z$ ) Data for Complexes 6–23, and Elemental Analyses for 6, 13, and 21**

compd	reacn time	FAB <sup>+</sup> MS ([M <sup>+</sup> ] – Br)	elemental anal. (%)
6	inst <sup>a</sup>	562.04	calcd for C <sub>26</sub> H <sub>26</sub> N <sub>3</sub> RhBr <sub>2</sub> (640.95): 48.55 (C), 4.07 (H), 6.53 (N), 24.85 (Br) found: 48.62 (C), 4.15 (H), 6.39 (N), 24.78 (Br)
7	5 min	576.05	
8	15 min	590.07	
9	30 min	604.08	
10	1 h	618.10	
11	1 h	632.12	
12	1 h	660.15	
13	12 h	688.18	calcd for C <sub>35</sub> H <sub>44</sub> N <sub>3</sub> RhBr <sub>2</sub> (796.52): 54.63 (C), 5.76 (H), 5.46 (N), 20.77 (Br) found: 54.56 (C), 5.70 (H), 5.49 (N), 20.69 (Br)
14	5 min	574.04	
15	5 min	588.05	
16	5 min	602.07	
17	30 min	602.07	
18	1 h	616.08	
19	2 h	630.10	
20	2 h	660.15	
21	12 h	700.18	calcd for C <sub>36</sub> H <sub>44</sub> N <sub>3</sub> RhBr <sub>2</sub> (779.10): 55.33 (C), 5.86 (H), 5.38 (N), 20.45 (Br) found: 55.24 (C), 5.61 (H), 5.35 (N), 20.56 (Br)
22	72 h	624.05	624.05
23	inst	640.07	640.07
24	inst		

<sup>a</sup> inst = instantaneously.

first spectrum was recorded after 2 min reaction time. 1-Bromodecane shows no absorption in the relevant visible region.

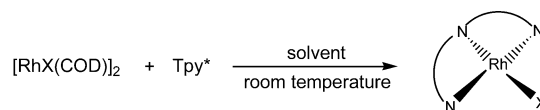
**Monitoring the Formation of Complex 13 with UV/Vis Spectroscopy in the Presence of 2-Methylphenol.** A standard cuvette was filled with 4 mL of an ethanolic solution of complex 2 ( $5.75 \times 10^{-5}$  M) and 1 g of 2-methylphenol (ca. 40 equiv) under an inert nitrogen atmosphere (glovebox). To this solution was added 2.4  $\mu$ L of 1-bromodecane (50 equiv) for the oxidative addition reaction, which was monitored with an HP8453 diode-array spectrophotometer at 298 K. In total, 90 electronic absorption spectra were recorded with a 60 s interval between each single measurement (5400 s total measuring time). The first spectrum was recorded after 1 min and 50 s reaction time. 2-Methylphenol shows no absorption in the relevant visible region.

## Results

**Syntheses of Complexes 1–24.** For the synthesis of complex 1 various solvents can be used (e.g. toluene, benzene, THF, and EtOH), while the synthesis of complex 2 is found to be the most successful when using EtOH as the solvent (Scheme 1). Complexes 1 and 2 are highly air sensitive, like the Rh(I) terpyridine complexes described in ref 89. They react with oxygen instantly to form mixtures of uncharacterized red Rh(III) species, as evidenced by <sup>1</sup>H NMR measurements of the products.

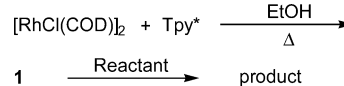
The synthesis of 2 in toluene and MeOH gave uncharacterized red products, while in THF uncharacterized pale yellow products were formed. The synthesis of 2 in benzene resulted in the formation of uncharacterized gray species. Hence, since EtOH is a suitable solvent for the syntheses of both complexes 1 and 2, all

### Scheme 1. Synthesis Procedure for Complexes 1 and 2

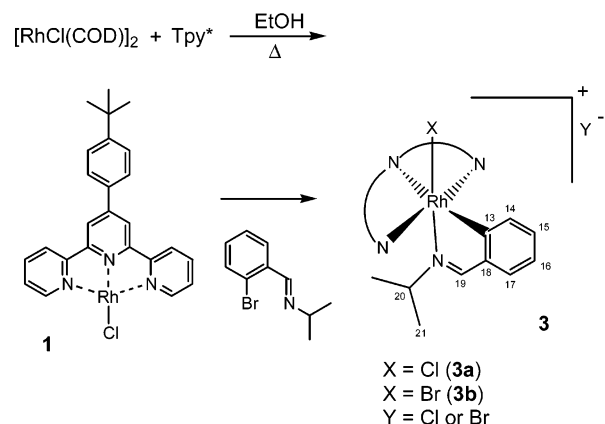


X = Cl for complex 1; solvent = toluene, benzene, THF, EtOH  
X = Br for complex 2; solvent = EtOH  
COD = 1,5-cyclooctadiene

### Scheme 2. Reaction Procedure of 1 with CHCl<sub>3</sub> and CH<sub>2</sub>Cl<sub>2</sub>



### Scheme 3. Reaction Procedure of 1 with (2-Bromobenzylidene)isopropylamine



oxidative addition reactions involving complexes 1 and 2 were performed in situ in EtOH.

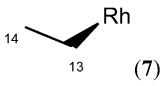
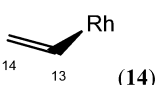

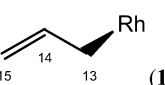
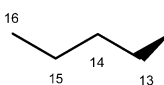
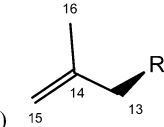
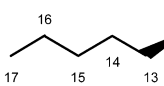
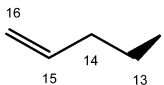
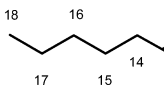
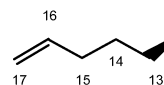
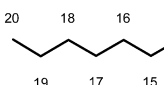
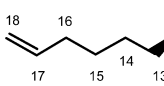
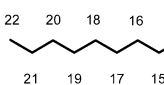
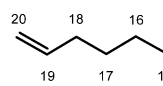
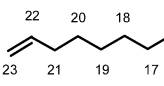
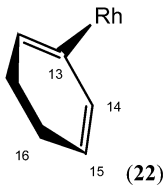
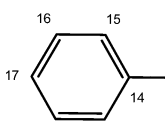
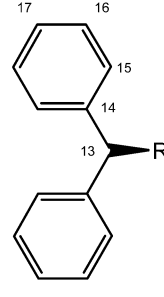
Initially, oxidative addition reactions with complex 1 (ca. 0.01 mmol) and 1–1000 equiv of CHCl<sub>3</sub> and CH<sub>2</sub>Cl<sub>2</sub> (Scheme 2) were studied.

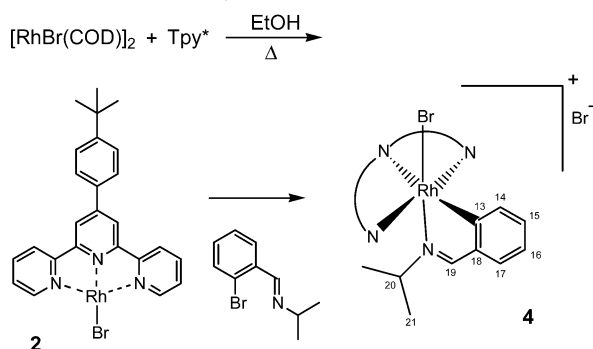
Unfortunately, the oxidative addition reactions involving 1 and chloroform or dichloromethane gave only mixtures of uncharacterized products. This is also the case in reactions of 1 with O<sub>2</sub>, HCl, C<sub>2</sub>Cl<sub>6</sub>, benzyl chloride, (2-chlorobenzylidene)isopropylamine, silicon chlorides, benzyl bromide, and MeBr. However, in the oxidative addition reaction of 1 and (2-bromobenzylidene)isopropylamine two isomeric products (Scheme 3) were formed, which could be identified by means of NMR techniques and mass spectrometry.

The majority of the <sup>1</sup>H signals of the two isomers of 3 in the NMR spectrum of the product mixture are overlapping each other. Only two pairs of nonoverlapping signals indicate the presence of two different species in the measured sample (Figure 1). The presence of two different compounds in the product mixture is also confirmed by FAB mass measurement. Masses of  $m/z$  649.16 and 693.11 are detected, representative for 3a ([M<sup>+</sup>] – Br) and 3b ([M<sup>+</sup>] – Cl), respectively. The composition of the product mixture is 3a:3b = 30:70 according to the <sup>1</sup>H NMR integrals.

To avoid the formation of mixtures, (2-bromobenzylidene)isopropylamine was oxidatively added to the complex [Rh<sup>I</sup>(Br)(Tpy<sup>\*</sup>)] (2). As expected, this reaction gave only one product, [(2-N-isopropyliminophenyl)-(Tpy<sup>\*</sup>)Rh<sup>III</sup>Br]<sup>+</sup>Br<sup>-</sup> (4) (Scheme 4).

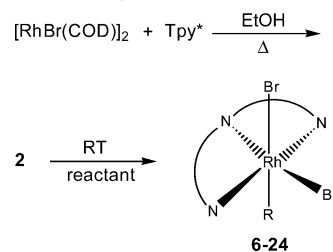
**Table 3. Atom Numbering of Complexes 6–24**

Saturated	Unsaturated
Me(C13)-Rh (6)	
 (7)	 (14)
 (8)	 (15)
 (9)	 (16)
 (10)	 (17)
 (11)	 (18)
 (12)	 (19)
 (13)	 (20)
	 (21)
	 (22)
	 (23)
	 (24)

**Scheme 4. Reaction Procedure of 2 with 2-(Isopropylimino)bromobenzene**

This success prompted us to perform oxidative addition reactions with complex **2** and ca. 100 equiv of various alkyl bromides (Table 1). As indicated earlier, all reactions were carried out in situ using EtOH as the solvent (Scheme 5). The atom numbering of complexes **6–24** is shown in Table 3, while reaction time and mass and elemental analyses of complexes **6–24** are summarized in Table 2.

**$^{15}\text{N}$  NMR Spectroscopy of Complex 4, Tpy\*, and 2-(Isopropylimino)bromobenzene.** The  $\delta(^{15}\text{N})$  signal of complex **4** has significantly shifted upfield compared to the  $\delta(^{15}\text{N})$  signal for the free ligands (Table 6). This

**Scheme 5. Reaction Procedure of 2 with ca. 100 Equiv of Alkyl Bromide Reactants**

means that all nitrogen atoms of **4** are coordinated to the rhodium metal. In view of this finding and the elemental composition of complex **4**, it is likely that it is an octahedral ionic Rh(III)–terpyridine complex with a bromide acting as a counteranion, as indicated in Scheme 4.

**$^{103}\text{Rh}$  NMR Spectroscopy of Complexes 4–7, 9, 13–17, and 22.** Transition-metal NMR shifts can nowadays easily be measured by modern 2D pulse techniques and serve as a probe into electronic and steric effects of ligands and substituents in metal complexes.<sup>90</sup> The influence of these effects on  $\delta(^{103}\text{Rh})$  for complexes **4–7, 9, 13–17, 22**, and  $[(\text{R}^3)\text{Rh}^{\text{III}}(\text{Cl})_2(2,6-$

(90) Von Philipsborn, W. *Chem. Soc. Rev.* **1999**, *28*, 95–105.

Table 4.  $^1H$  NMR Data of Complexes 6–24<sup>a</sup>

compd	$^1H$ NMR ( $\delta$ )
<b>6</b>	9.53 (d, 5.4 Hz, 2H (6,6'')), 8.24 (s, 2H(3',5')), 8.21 (d, 8.1 Hz, 2H (3,3'')), 8.00 (t, 7.8 Hz, 2H (4,4'')), 7.76 (d, 8.7 Hz, 2H (8,8')), 7.60 (d, 9 Hz, 2H (9,9')), 7.59 (m, 2H (5,5')), 1.41 (s, 9H ( <i>t</i> -Bu)), 1.11 (d, $^2J(Rh,H) = 2.4$ Hz, 3H (13))
<b>7</b>	9.53 (d, 5.5 Hz, 2H (6,6'')), 8.28 (s, 2H (3',5')), 8.25 (d, 8.0 Hz, 2H (3,3'')), 8.02 (t, 7.8 Hz, 2H (4,4'')), 7.81 (d, 8.5 Hz, 2H (8,8')), 7.63 (d, 8.5 Hz, 2H (9,9')), 7.62 (m, 2H (5,5'')), 2.22 (dq, $^3J(H,H) = 7.5$ Hz, $^2J(Rh,H) = 3$ Hz, 2H (13)), 1.44 (s, 9H ( <i>t</i> -Bu)), 0.22 (t, 7.5 Hz, 3H (14))
<b>8</b>	9.45 (d, 5.5 Hz, 2H (6,6'')), 8.25 (s, 2H (3',5')), 8.22 (d, 7.5 Hz, 2H (3,3'')), 8.02 (t, 7.8 Hz, 2H (4,4'')), 7.79 (d, 8.5 Hz, 2H (8,8')), 7.62 (d, 8.5 Hz, 2H (9,9')), 7.60 (t, 7.5 Hz, 2H (5,5'')), 2.17 (dt, $^3J(H,H) = 8.5$ Hz, $^2J(Rh,H) = 2.5$ Hz, 2H (13)), 1.43 (s, 9H ( <i>t</i> -Bu)), 0.63 (m, 8.5 Hz, 2H (14)), 0.58 (t, 6.8 Hz, 3H (15))
<b>9</b>	9.47 (d, 5.4 Hz, 2H (6,6'')), 8.23 (d, 7.6 Hz, 2H (3,3'')), 8.21 (s, 2H (3',5')), 7.90 (t, 7.1 Hz, 2H (4,4'')), 7.76 (d, 8.4 Hz, 2H (8,8')), 7.53 (t, 6.5 Hz, 2H (5,5'')), 7.52 (d, 8.7 Hz, 2H (9,9')), 2.06 (dt, $^3J(H,H) = 8.6$ Hz, $^2J(Rh,H) = 2.7$ Hz, 2H (13)), 1.40 (s, 9H ( <i>t</i> -Bu)), 0.91 (m, 7.4 Hz, 2H (14)), 0.48 (m, 2 + 3H)
<b>10</b>	9.48 (d, 5.4 Hz, 2H (6,6'')), <sup>b</sup> 8.24 (d, 6.9 Hz, 2H (3,3'')), <sup>b</sup> 8.23 (s, 2H (3',5')), 7.93 (t, 7.8 Hz, 2H (4,4'')), <sup>b</sup> 7.77 (d, 8.7 Hz, 2H (8,8')), <sup>b</sup> 7.56 (t, 7.0 Hz, 2H (5,5'')), <sup>b</sup> 7.54 (d, 8.7 Hz, 2H (9,9')), <sup>b</sup> 2.07 (dt, $^3J(H,H) = 8.6$ Hz, $^2J(Rh,H) = 2.7$ Hz, 2H (13)), 1.41 (s, 9H ( <i>t</i> -Bu)), 0.90 (m, 2 $\times$ 2H), 0.55 (m, 2H + 3H)
<b>11</b>	9.49 (d, 5.5 Hz, 2H (6,6'')), 8.28 (d, 8.0 Hz, 2H (3,3'')), 8.23 (s, 2H (3',5')), 7.90 (t, 7.8 Hz, 2H (4,4'')), 7.79 (d, 8.0 Hz, 2H (8,8')), 7.56 (t, 6.0 Hz, 2H (5,5'')), 7.52 (d, 8.0 Hz, 2H (9,9')), 2.08 (dt, $^3J(H,H) = 7.5$ Hz, $^2J(Rh,H) = 2.5$ Hz, 2H (13)), 1.42 (s, 9H ( <i>t</i> -Bu)), 0.95 (m, 7.0 Hz, 2H (14)), 0.88 (m, 2 $\times$ 2H), 0.65 (t, 7 Hz, 3H (17)), 0.52 (m, 7.5 Hz, 2H (16))
<b>12</b>	9.50 (d, 5.4 Hz, 2H (6,6'')), 8.25 (d, 7.8 Hz, 2H (3,3'')), 8.24 (s, 2H (3',5')), 7.95 (t, 8.0 Hz, 2H (4,4'')), 7.79 (d, 8.0 Hz, 2H (8,8')), 7.58 (t, 7.4 Hz, 2H (5,5'')), 7.57 (d, 8.0 Hz, 2H (9,9')), 2.10 (dt, $^3J(H,H) = 7.8$ Hz, $^2J(Rh,H) = 2.8$ Hz, 2H (13)), 1.43 (s, 9H ( <i>t</i> -Bu)), 1.12 (m, 2H), 1.03 (m, 2H), 0.91 (m, 3 $\times$ 2H), 0.76 (t, 7.0 Hz, 2H (20)), 0.65 (m, 2H)
<b>13</b>	9.50 (d, 5.7 Hz, 2H (6,6'')), 8.25 (d, 8.1 Hz, 2H (3,3'')), 8.24 (s, 2H (3',5')), 7.95 (t, 8.1 Hz, 2H (4,4'')), 7.79 (d, 8.4 Hz, 2H (8,8')), 7.57 (t, 7.4 Hz, 2H (5,5'')), 7.56 (d, 8.4 Hz, 2H (9,9')), 2.10 (dt, $^3J(H,H) = 8.6$ Hz, $^2J(Rh,H) = 2.6$ Hz, 2H (13)), 1.43 (s, 9H ( <i>t</i> -Bu)), 1.21 (m, 7.05 Hz, 2H (14)), 1.09 (m, 4 $\times$ 2H), 0.90 (m, 2 $\times$ 2H), 0.81 (t, 6.8 Hz, 3H (22)), 0.55 (m, 2H)
<b>14</b>	9.52 (d, 5.4 Hz, 2H (6,6'')), 8.25 (s, 2H (3',5')), 8.23 (d, 6.6 Hz, 2H (3,3'')), 8.00 (t, 7.8 Hz, 2H (4,4'')), 7.76 (d, 8.4 Hz, 2H (8,8')), 7.60 (t, 6.7 Hz, 2H (5,5'')), 7.59 (d, 8.7 Hz, 2H (9,9')), 7.22 (ddd, $^3J(H,H(trans) = 15.9$ Hz, $^3J(H,H(cis) = 3.6$ Hz, 1H (13)), 4.55 (d, 6.6 Hz, 1H (14-cis)), 3.72 (d, 16.8 Hz, 1H (14-trans)), 1.41 (s, 9H ( <i>t</i> -Bu))
<b>15</b>	9.45 (d, 5.5 Hz, 2H (6,6'')), 8.24 (s, 2H (3',5')), 8.21 (d, 7.5 Hz, 2H (3,3'')), 8.00 (t, 7.8 Hz, 2H (4,4'')), 7.78 (d, 8.5 Hz, 2H (8,8')), 7.61 (d, 9.0 Hz, 2H (9,9')), 7.60 (t, 8.0 Hz, 2H (5,5'')), 5.28 (m, 1H (14)), 4.32 (d, 10.0 Hz, 1H (15-cis)), 4.20 (d, 17.5 Hz, 1H (15-trans)), 2.97 (dd, $^3J(H,H) = 8.5$ Hz, $^2J(Rh,H) = 3.0$ Hz, 2H (13)), 1.43 (s, 9H ( <i>t</i> -Bu))
<b>16</b>	9.54 (d, 5.5 Hz, 2H (6,6'')), 8.25 (s, 2H (3',5')), 8.24 (d, 8.5 Hz, 2H (3,3'')), 7.97 (t, 7.5 Hz, 2H (4,4'')), 7.80 (d, 8.5 Hz, 2H (8,8')), 7.61 (d, 8.5 Hz, 2H (9,9')), 7.58 (t, 6.8 Hz, 2H (5,5'')), 4.15 (s, 1H (15-cis)), 3.63 (s, 1H (15-trans)), 3.02 (d, $^2J(Rh,H) = 3.0$ Hz, 2H (13)), 1.45 (s, 9H ( <i>t</i> -Bu)), 1.15 (s, 3H (16))
<b>17</b>	9.47 (d, 5.0 Hz, 2H (6,6'')), 8.24 (d, 7.0 Hz, 2H (3,3'')), 8.23 (s, 2H (3',5')), 7.97 (t, 7.8 Hz, 2H (4,4'')), 7.77 (d, 8.5 Hz, 2H (8,8')), 7.58 (t, 6.8 Hz, 2H (5,5'')), 7.57 (d, 8.5 Hz, 2H (9,9')), 5.43 (m, 1H (15)), 4.55 (m, 2H (16)), 2.10 (dt, $^3J(H,H) = 8.5$ Hz, $^2J(Rh,H) = 3.0$ Hz, 2H (13)), 1.43 (s, 9H ( <i>t</i> -Bu)), 1.41 (m, 2H (14))
<b>18</b>	9.46 (d, 5.5 Hz, 2H (6,6'')), 8.22 (d, 8.5 Hz, 2H (3,3'')), 8.23 (s, 2H (3',5')), 7.93 (t, 7.8 Hz, 2H (4,4'')), 7.78 (d, 8.5 Hz, 2H (8,8')), 7.56 (t, 7.0 Hz, 2H (5,5'')), 7.55 (d, 8.0 Hz, 2H (9,9')), 5.43 (m, 1H (16)), 4.63 (m, 2H (17)), 2.10 (dt, $^3J(H,H) = 8.8$ Hz, $^2J(Rh,H) = 2.5$ Hz, 2H (13)), 1.69 (psq, 7.0 Hz, 2H (15)), 1.43 (s, 9H ( <i>t</i> -Bu)), 0.68 (m, 2H (14))
<b>19</b>	9.50 (d, 5.5 Hz, 2H (6,6'')), 8.25 (s, 2H (3',5')), 8.24 (d, 8.0 Hz, 2H (3,3'')), 7.98 (t, 8.0 Hz, 2H (4,4'')), 7.79 (d, 8.5 Hz, 2H (8,8')), 7.60 (t, 7.0 Hz, 2H (5,5'')), 7.58 (d, 8.0 Hz, 2H (9,9')), 5.48 (m, 1H (17)), 4.66 (m, 2H (18)), 2.10 (dt, $^3J(H,H) = 8.5$ Hz, $^2J(Rh,H) = 3.0$ Hz, 2H (13)), 1.69 (psq, 7.2 Hz, 2H (16)), 1.43 (s, 9H ( <i>t</i> -Bu)), 1.03 (m, 2H (15)), 0.56 (m, 2H (14))
<b>20</b>	9.50 (d, 5.1 Hz, 2H (6,6'')), 8.24 (s, 2H (3',5')), 8.24 (d, 7.2 Hz, 2H (3,3'')), 7.96 (t, 7.8 Hz, 2H (4,4'')), 7.79 (d, 8.4 Hz, 2H (8,8')), 7.59 (t, 7.0 Hz, 2H (5,5'')), 7.57 (d, 8.1 Hz, 2H (9,9')), 5.64 (m, 1H (19)), 4.82 (m, 2H (20)), 2.09 (dt, $^3J(H,H) = 8.7$ Hz, $^2J(Rh,H) = 2.7$ Hz, 2H (13)), 1.81 (psq, 7.0 Hz, 2H (18)), 1.42 (s, 9H ( <i>t</i> -Bu)), 1.00 (m, 3 $\times$ 2H), 0.58 (m, 2H)
<b>21</b>	9.48 (d, 5.5 Hz, 2H (6,6'')), 8.29 (d, 7.5 Hz, 2H (3,3'')), 8.23 (s, 2H (3',5')), 7.87 (t, 8.0 Hz, 2H (4,4'')), 7.78 (d, 8.0 Hz, 2H (8,8')), 7.53 (t, 6.5 Hz, 2H (5,5'')), 7.49 (d, 8.5 Hz, 2H (9,9')), 5.74 (m, 1H (22)), 4.88 (m, 2H (23)), 2.07 (dt, $^3J(H,H) = 8.8$ Hz, $^2J(Rh,H) = 3.0$ Hz, 2H (13)), 1.92 (psq, 2H (21)), 1.42 (s, 9H ( <i>t</i> -Bu)), 1.22 (m, 2H), 1.09 (m, 2H), 1.02 (m, 2H), 0.90 (m, 3 $\times$ 2H), 0.51 (m, 2H)
<b>22</b>	9.53 (d, 5.5 Hz, 2H (6,6'')), 8.28 (s, 2H (3',5')), 8.23 (d, 8.0 Hz, 2H (3,3'')), 8.12 (t, 7.8 Hz, 2H (4,4'')), 7.76 (d, 7.5 Hz, 2H (8,8')), 7.68 (t, 6.3 Hz, 2H (5,5'')), 7.65 (d, 8.5 Hz, 2H (9,9')), 6.73 (m, 2 + 1H (15,16)), 6.65 (d, 7.5 Hz, 2H (14)), 1.41 (s, 9H ( <i>t</i> -Bu)); NOESY interaction was found between H(14) and H(6,6')
<b>23</b>	9.42 (d, 6.0 Hz, 2H (6,6'')), 8.63 (s, 2H (3',5')), 8.58 (d, 7.5 Hz, 2H (3,3'')), 8.27 (t, 7.4 Hz, 2H (4,4'')), 7.96 (d, 8.7 Hz, 2H (8,8')), 7.78 (t, 6.6 Hz, 2H (5,5'')), 7.70 (d, 9.0 Hz, 2H (9,9')), 6.83 (t, 7.4 Hz, 1H (17)), 6.58 (t, 8.1 Hz, 2H (16)), 6.32 (d, 7.5 Hz, 2H (15)), 3.79 (d, $^2J(Rh,H) = 2.7$ Hz, 2H (13)), 1.43 (s, 9H ( <i>t</i> -Bu))
<b>24</b>	9.06 (5.4 Hz, 2H (6,6'')), 8.09 (s, 2H (3',5')), 7.87 (d, 7.8 Hz, 2H (3,3'')), 7.78 (m, 2 + 2H), 7.62 (d, 8.4 Hz, 2H (9,9')), 7.28 (t, 6.6 Hz, 2H (16)), 6.82 (m, 2 + 2H (15)), 6.65 (t, 7.7 Hz, 2 + 2H (14)), 5.94 (d, $^2J(Rh,H) = 3.6$ Hz, 1H (13)), 1.42 (s, 9H ( <i>t</i> -Bu))

<sup>a</sup> For atom numbering cf. Table 2. All  $^1H$  NMR spectra were measured in  $CD_2Cl_2$  (except for **23**, in  $CD_3OD$ ). Complex **6** was measured with a Bruker AMX 300 spectrometer and complex **9** with a Bruker DRX 300 spectrometer; complexes **10**, **13**, **14**, **20**, **23**, and **24** were measured with a Varian Mercury 300 spectrometer and complexes **7**, **8**, **11**, **12**, **15–19**, **21**, and **22** with a Varian Inova 500 spectrometer.

<sup>b</sup> The assignment is based on 2D COSY measurements (Varian Inova 500), performed at room temperature.

$(C(R^1)=NR^2)_2C_5H_3N$ <sup>74</sup> has been studied with PFG HMQC  $^1H$  and  $^{103}Rh$  NMR techniques.

The  $\delta(^{103}Rh)$  values for complexes **4–7**, **9**, **13–17**, and **22** (Table 7) are comparable with the  $\delta(^{103}Rh)$  values for the similar complexes  $[(R^3)Rh^{III}(Cl)_2(2,6-(C(R^1)=NR^2)_2C_5H_3N)]$  for which  $^{103}Rh$  NMR data are available<sup>74,91</sup> (Table 8).

**Monitoring the Formation of Complex 13 with UV/Vis Spectroscopy.** Besides the electronic absorption spectra of isolated **2** and **13** (Figure 2), also the formation of complex **13** was monitored by means of UV/vis spectrometry (Figure 3). From the monitoring, two distinct isosbestic points can be observed in the absorp-



**Table 5.**  $^{13}\text{C}$  NMR Data of Complexes **6**–**22**<sup>a</sup>

compd	$^{13}\text{C}$ NMR ( $\delta$ )
<b>6</b>	157.08 (C2', C6'), 155.34 (C2, C2''), 155.00 (C10), 154.94 (C6, C6''), 150.00 (C4'), 138.36 (C4, C4''), 132.72 (C7), 127.96 (C5, C5''), 127.67 (C8, C8'), 126.89 (C9, C9'), 124.09 (C3, C3''), 120.33 (C3', C5'), 35.29 (C11), 31.39 (C12, C12', C12''), 8.39 (d, $^1J(\text{Rh},\text{C13}) = 21.14$ Hz)
<b>7</b>	157.15 (C2', C6'), 155.68 (C2, C2''), 155.24 (C6, C6''), 155.19 (C10), 150.75 (C4'), 138.74 (C4, C4''), 133.44 (C7), 128.39 (C5, C5''), 127.78 (C8, C8'), 126.19 (C9, C9'), 123.97 (C3, C3''), 120.79 (C3', C5'), 35.48 (C11), 31.53 (C12, C12', C12''), 24.38 (d, $^1J(\text{Rh},\text{C13}) = 21.25$ Hz), 17.09 (C14)
<b>8</b>	157.21 (C2', C6'), 155.72 (C2, C2''), 155.26 (C6, C6''), 155.20 (C10), 150.84 (C4'), 138.76 (C4, C4''), 133.50 (C7), 128.40 (C5, C5''), 127.78 (C8, C8'), 126.18 (C9, C9'), 123.96 (C3, C3''), 120.80 (C3', C5'), 35.48 (C11), 33.12 (d, $^1J(\text{Rh},\text{C13}) = 21.75$ Hz), 31.52 (C12, C12', C12''), 25.57, 15.29
<b>9</b>	156.81 (C2', C6'), 155.27 (C2, C2''), 154.80 (C6, C6''), 154.80 (C10), 149.71 (C4'), 138.20 (C4, C4''), 132.58 (C7), 127.83 (C5, C5''), 127.46 (C8, C8'), 126.69 (C9, C9'), 123.73 (C3, C3''), 120.13 (C3', C5'), 35.10 (C11), 34.10, 31.16 (C12, C12', C12''), 30.07 (d, $^1J(\text{Rh},\text{C13}) = 21.25$ Hz), 23.96, 13.48
<b>10</b>	156.85 (C2', C6'), <sup>c</sup> 155.24 (C2, C2''), <sup>c</sup> 154.79 (C6, C6''), <sup>b</sup> 154.73 (C10), <sup>c</sup> 149.30 (C4'), <sup>c</sup> 138.02 (C4, C4''), <sup>b</sup> 132.41 (C7), <sup>c</sup> 127.72 (C5, C5''), <sup>b</sup> 127.54 (C8, C8'), <sup>b</sup> 126.61 (C9, C9'), <sup>b</sup> 123.82 (C3, C3''), <sup>b</sup> 120.02 (C3', C5'), <sup>b</sup> 35.11 (C11), <sup>c</sup> 33.20, 31.37, 31.21 (C12, C12', C12''), <sup>c</sup> 30.19 (d, $^1J(\text{Rh},\text{C13}) = 21.25$ Hz), 22.26, 13.75
<b>11</b>	157.16 (C2', C6'), 155.57 (C2, C2''), 155.13 (C6, C6''), 155.05 (C10), 149.68 (C4'), 138.37 (C4, C4''), 132.82 (C7), 128.09 (C5, C5''), 127.87 (C8, C8'), 126.97 (C9, C9'), 124.13 (C3, C3''), 120.39 (C3', C5'), 35.46 (C11), 32.09, 31.85, 31.55 (C12, C12', C12''), 31.11, 30.76 (d, $^1J(\text{Rh},\text{C13}) = 21.30$ Hz), 22.99, 14.21
<b>12</b>	156.85 (C2', C6'), 155.24 (C2, C2''), 154.87 (C6, C6''), 154.73 (C10), 149.32 (C4'), 138.01 (C4, C4''), 132.44 (C7), 127.72 (C5, C5''), 127.53 (C8, C8'), 126.62 (C9, C9'), 123.80 (C3, C3''), 120.01 (C3', C5'), 35.11 (C11), 31.83, 31.75, 31.21 (C12, C12', C12''), 31.05, 30.26 (d, $^1J(\text{Rh},\text{C13}) = 20.63$ Hz), 29.22, 29.19, 22.68, 13.92
<b>13</b>	156.82 (C2', C6'), 155.23 (C2, C2''), 154.82 (C6, C6''), 154.69 (C10), 149.43 (C4'), 137.98 (C4, C4''), 132.59 (C7), 127.73 (C5, C5''), 127.47 (C8, C8'), 126.64 (C9, C9'), 123.68 (C3, C3''), 120.05 (C3', C5'), 35.08 (C11), 31.96, 31.73, 31.18 (C12, C12', C12''), 31.05, 30.22 (d, $^1J(\text{Rh},\text{C13}) = 21.25$ Hz), 29.57, 29.36, 29.23, 29.19, 22.76, 13.98
<b>14</b>	156.79 (C2', C6'), 155.04 (C2, C2''), 155.01 (C10), 154.83 (C6, C6''), 151.28 (C4'), 147.86 (d, $^1J(\text{Rh},\text{C13}) = 26.88$ Hz), 138.80 (C4, C4'), 132.95 (C7), 128.12 (C5, C5''), 127.45 (C8, C8'), 126.89 (C9, C9'), 123.97 (C3, C3''), 120.63 (C3', C5'), 116.45 (C14), 35.12 (C11), 31.13 (C12, C12', C12'')
<b>15</b>	157.21 (C2', C6'), 155.67 (C2, C2''), 155.29 (C10), 155.21 (C6, C6''), 150.83 (C4'), 143.85 (C15), 138.81 (C4, C4''), 133.34 (C7), 128.38 (C5, C5''), 127.78 (C8, C8'), 126.20 (C9, C9'), 124.25 (C3, C3''), 120.82 (C3', C5'), 111.05 (C14), 35.49 (C11), 31.52 (C12, C12', C12''), 29.74 (d, $^1J(\text{Rh},\text{C13}) = 19.50$ Hz)
<b>16</b>	157.10 (C2', C6'), 155.43 (C2, C2''), 154.98 (C6, C6''), 154.71 (C10), 151.41 (C4'), 149.90 (C15), 138.08 (C4, C4''), 133.06 (C7), 127.51 (C5, C5''), 127.42 (C8, C8'), 126.77 (C9, C9'), 123.85 (C3, C3''), 120.19 (C3', C5'), 108.00 (C14), 35.11 (C11), 34.06 (d, $^1J(\text{Rh},\text{C13}) = 20.00$ Hz), 31.19 (C12, C12', C12''), 23.25 (C16)
<b>17</b>	157.24 (C2', C6'), 155.69 (C2, C2''), 155.24 (C10), 155.24 (C6, C6''), 150.53 (C4'), 139.32 (C16), 138.75 (C4, C4''), 133.12 (C7), 128.37 (C5, C5''), 127.83 (C8, C8'), 126.21 (C9, C9'), 124.10 (C3, C3''), 120.68 (C3', C5'), 113.37 (C15), 36.28 (C14), 35.49 (C11), 31.54 (C12, C12', C12''), 28.22 (d, $^1J(\text{Rh},\text{C13}) = 23.00$ Hz)
<b>18</b>	157.19 (C2', C6'), 155.63 (C2, C2''), 155.23 (C10), 155.19 (C6, C6''), 150.14 (C4'), 139.03 (C17), 138.65 (C4, C4''), 132.89 (C7), 128.26 (C5, C5''), 127.87 (C8, C8'), 126.22 (C9, C9'), 124.20 (C3, C3''), 120.55 (C3', C5'), 114.05 (C16), 35.49 (C11), 35.33, 31.55 (C12, C12', C12''), 29.84 (d, $^1J(\text{Rh},\text{C13}) = 21.25$ Hz), 29.84
<b>19</b>	157.15 (C2', C6'), 155.59 (C2, C2''), 155.26 (C6, C6''), 155.02 (C10), 150.19 (C4'), 139.46 (C18), 138.41 (C4, C4''), 133.36 (C7), 128.20 (C5, C5''), 127.79 (C8, C8'), 127.10 (C9, C9'), 123.90 (C3, C3''), 120.58 (C3', C5'), 114.14 (C17), 35.45 (C11), 33.72, 31.53 (C12, C12', C12''), 31.48, 30.35, 29.87 (d, $^1J(\text{Rh},\text{C13}) = 21.25$ Hz)
<b>20</b>	156.85 (C2', C6'), 155.23 (C2, C2''), 154.76 (C6, C6''), 154.76 (C10), 149.22 (C4'), 139.35 (C20), 138.03 (C4, C4''), 132.29 (C7), 127.41 (C5, C5''), 127.56 (C8, C8'), 126.56 (C9, C9'), 123.88 (C3, C3''), 119.99 (C3', C5'), 113.83 (C19), 35.11 (C11), 33.69, 31.65, 31.22 (C12, C12', C12''), 30.86, 30.14 (d, $^1J(\text{Rh},\text{C13}) = 21.13$ Hz), 28.89, 28.71
<b>21</b>	156.86 (C2', C6'), 155.23 (C2, C2''), 154.76 (C6, C6''), 154.76 (C10), 149.18 (C4'), 139.47 (C23), 138.02 (C4, C4''), 132.26 (C7), 127.70 (C5, C5''), 127.56 (C8, C8'), 126.59 (C9, C9'), 123.89 (C3, C3''), 119.96 (C3', C5'), 113.92 (C22), 35.11 (C11), 33.88, 31.72, 31.22 (C12, C12', C12''), 31.02, 30.26 (d, $^1J(\text{Rh},\text{C13}) = 20.63$ Hz), 29.49, 29.17, 29.21, 29.17, 29.02
<b>22</b>	156.86 (C2', C6'), 155.23 (C2, C2''), 154.76 (C6, C6''), 154.76 (C10), 149.18 (C4'), 139.47 (C23), 138.02 (C4, C4''), 132.26 (C7), 127.70 (C5, C5''), 127.56 (C8, C8'), 126.59 (C9, C9'), 123.89 (C3, C3''), 119.96 (C3', C5'), 113.92 (C22), 35.11 (C11), 33.88, 31.72, 31.22 (C12, C12', C12''), 31.02, 30.26 (d, $^1J(\text{Rh},\text{C13}) = 20.63$ Hz), 29.49, 29.17, 29.21, 29.17, 29.02

<sup>a</sup> For atom numbering, cf. Table 2. All  $^{13}\text{C}$  NMR spectra were measured in  $\text{CD}_2\text{Cl}_2$  and recorded at 125 MHz with a Varian Inova 500 spectrometer. <sup>b</sup> These NMR assignments are based on 2D HETCOR measurements (Varian Inova 500), performed at room temperature. <sup>c</sup> These NMR assignments are based on mathematical simulations.

tion spectra of the oxidative addition reaction (Figure 3). Monitoring the formation of complex **13** in the presence of 2-methylphenol (*o*-cresol) rendered absorption spectra similar to those observed without 2-methylphenol.

## Discussion

**Syntheses of Complexes 1–24.** Like the syntheses of the complexes  $[\text{Rh}^{\text{I}}(\text{X})(2,2':6',2''\text{-terpyridine})]$  ( $\text{X} = \text{Cl}, \text{Br}$ ), as described in ref 89, the syntheses of complexes **1** and **2** (blue) were rather simple once the right reaction conditions were found. Complexes **1** and **2** are air sensitive and form red Rh(III) species in air.

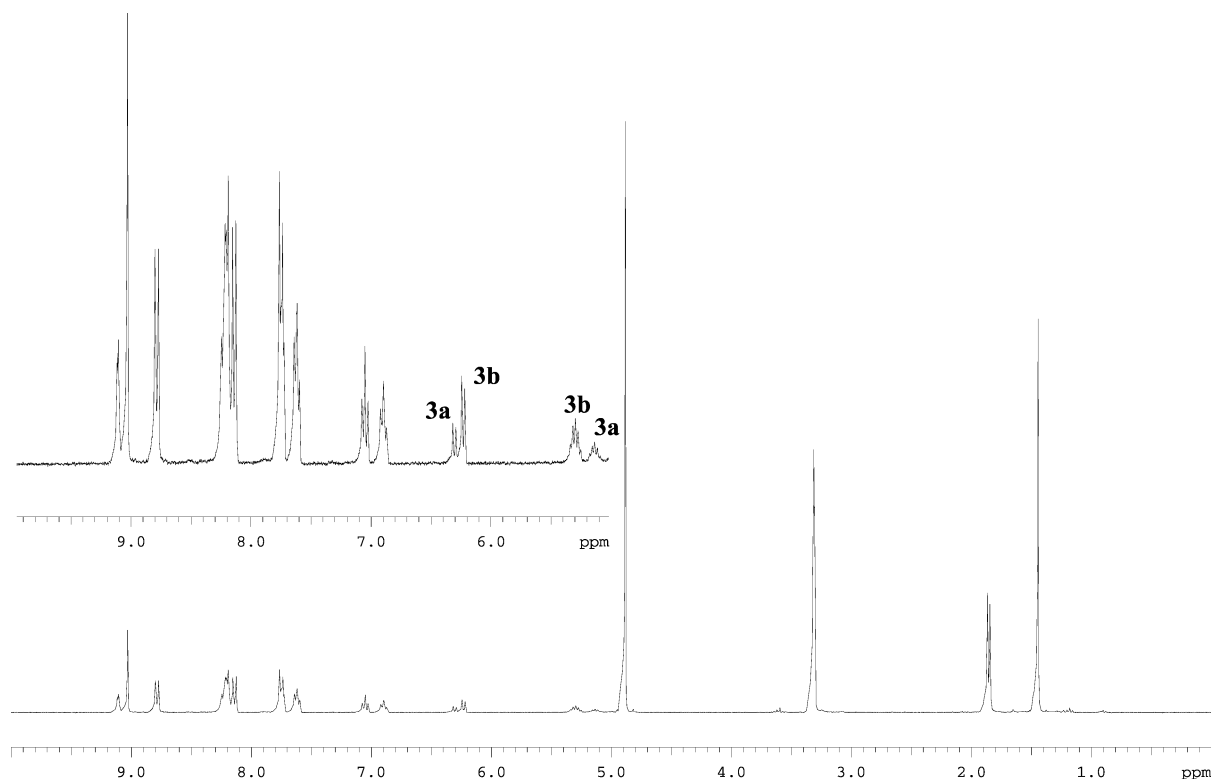
Various oxidative addition reactions with **1** and carbon–chloride bonds gave mixtures of uncharacterized products. On the basis of  $^1\text{H}$  NMR studies (only broad signals) and mass measurements (only the frag-

ment  $[\text{Rh}(\text{Cl})(\text{Tpy}^*)]$  could be detected with some certainty), it is impossible to characterize the different products. It is likely that one side product is a Rh(III) trichloride species. It is known that oxidative addition reactions between Rh(I) chlorides and alkyl chlorides, in particular  $\text{CH}_2\text{Cl}_2$  and  $\text{CHCl}_3$ , in EtOH can also give Rh(III) trichloride species as decomposition products together with diethoxyalkyl compounds.<sup>69</sup>

Furthermore, the oxidative addition reactions with **1** and carbon–bromide bonds also gave mixtures of uncharacterized products, except when 2-(isopropylimino)-bromobenzene was used as reactant, forming a mixture of complexes **3a** and **3b**. The reaction between complex **2** and 2-(isopropylimino)bromobenzene gave the single product complex **4**. The  $^1\text{H}$  chemical shifts of complexes **3b** and **4** are identical.

Similar to the synthesis of complex **4**, oxidative





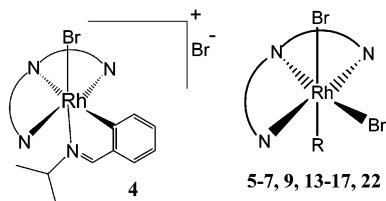
**Figure 1.**  $^1H$  NMR spectrum at 300 MHz of the isolated mixture **3a** + **3b**.

**Table 6.**  $^{15}N$  Chemical Shifts of Complex **4**,  $Tpy^*$ , and (2-Bromobenzylidene)isopropylamine

$^{15}N$ chem shift <sup>a</sup>		
<b>4</b> (in $CD_3OD$ )	$Tpy^*$ (in $CD_2Cl_2$ )	(2-bromobenzylidene)-isopropylamine
-151.92 (N1, N1')	-85.39 (N1)	-34.27 (in $CD_3OD$ )
-140.44 (N1')	-71.35 (N1, N1')	-23.54 (in $CD_2Cl_2$ )
-112.16 (N2)		

<sup>a</sup> In ppm, measured at room temperature.

**Table 7.**  $^{103}Rh$  Chemical Shifts in  $CD_2Cl_2$ , Measured at Room Temperature<sup>a</sup>

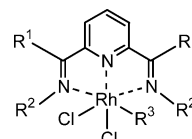


complex (R)	$\delta$ (ppm)	complex (R)	$\delta$ (ppm)
<b>4</b> <sup>a</sup>	3221	<b>14</b> (ethenyl)	3415
<b>5</b> (Br)	4540	<b>15</b> (2-propenyl)	3533
<b>6</b> (Me)	3366	<b>16</b> (2-methyl-2-propenyl)	3545
<b>7</b> (Et)	3365	<b>17</b> (3-butenyl)	3396
<b>9</b> (Bu)	3380	<b>22</b> (Ph)	3548
<b>13</b> (decyl)	3375		

<sup>a</sup> Measured in  $CD_3OD$  at room temperature.

addition reactions in EtOH with complex **2** and various bromohydrocarbons gave clean products (complexes **5–24**) in almost quantitative yields. In contrast to the dark blue complexes **1** and **2**, all synthesized Rh(III) terpyridine species are air stable and yellow. Primary  $sp^3$  and vinylic  $sp^2$  carbon–bromide bonds reacted more quickly with complex **2** than the  $sp^2$  carbon–bromide

**Table 8.**  $^{103}Rh$  Chemical Shifts in  $CD_2Cl_2$ , Measured at Room Temperature<sup>a</sup>



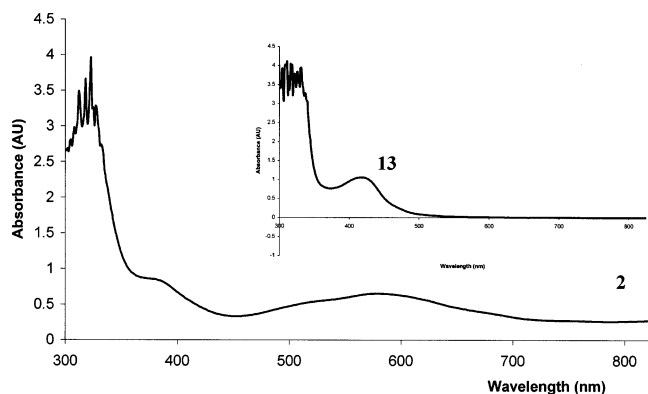
compd <sup>74</sup>	R <sup>1</sup>	R <sup>2</sup>	R <sup>3</sup>	$\delta$ (ppm) <sup>91</sup>
<b>A</b>	H	<i>i</i> -Pr	$CH_2Cl$	3570
<b>B</b>	H	Cy	$CH_2Cl$	3569
<b>C</b>	H	<i>t</i> -Bu	$CH_2Cl$	4121
<b>D</b>	H	<i>p</i> -A	$CH_2Cl$	3654
<b>E</b>	$CH_3$	<i>p</i> -A	$CH_2Cl$	3561
<b>F</b>	H	<i>i</i> -Pr	$CH_2Ph$	3649
<b>G</b>	H	<i>i</i> -Pr	Cl	4923

<sup>a</sup> Abbreviations: *i*-Pr = *i*propyl; Cy = cyclohexyl; *t*-Bu = *tert*-butyl; *p*-A = *p*-anisyl.

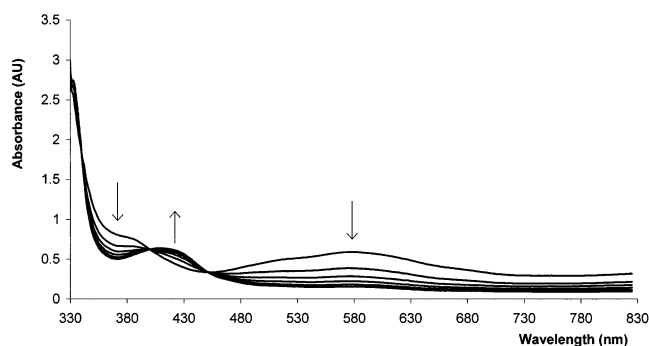
bond of bromobenzene, as indicated by their reaction time (Table 3). Furthermore, generally, smaller saturated and terminal unsaturated alkyl bromides reacted more quickly than the larger ones (Table 3). Under the applied reaction conditions (see the Experimental Section), only bromomethane, benzyl bromide, and diphenylbromomethane reacted instantaneously with complex **2**.

Complexes **5–24** dissolved sufficiently to excellently in (deuterated) dichloromethane and rather poorly in (deuterated) methanol. In contrast, complexes **3a,b** and **4** dissolved very well in (deuterated) methanol and not at all in (deuterated) dichloromethane. Their charged character could be the reason for the high solubility of the last three complexes in methanol.

**Geometry of Complexes 3–24.** Since attempts to grow crystals of complexes **3–24** failed, the determina-



**Figure 2.** Electronic absorption spectra of complexes **2** and **13** in ethanol.



**Figure 3.** UV-vis reaction spectrum of the oxidative addition reaction of complex **2** with 1-bromodecane in EtOH.

tion of their geometry is based on their  $^1\text{H}$  and  $^{13}\text{C}$  NMR spectra, the  $^{15}\text{N}$  NMR experiments of complex **4**, and NOE 2D ( $^1\text{H}$ ) NMR experiments of complex **22**.

The  $\delta(^{15}\text{N})$  signals for complex **4** ( $-112.16$ ,  $-140.55$ , and  $-151.92$  ppm) is not too different from the  $\delta(^{15}\text{N})$  signals for the complexes  $[\text{Pd}(\text{N}-\text{N})_2(\text{CH}_3)][\text{X}]$  ( $\text{N}-\text{N} = 1,10$ -phenanthroline (phen), 3,4,7,8-tetramethyl-1,10-phenanthroline (tm-phen);  $\text{X} = \text{OTf}$  (triflate),  $\text{PF}_6^-$ ;  $\delta(^{15}\text{N}) -123.6$  and  $-130.8$  ppm for phen and tm-phen derivatives, respectively) described by Milani et al.<sup>87</sup> The coordination shifts, i.e. the differences in  $\delta(^{15}\text{N})$  between the free ligands and the relevant complexes **4** and  $[\text{Pd}(\text{N}-\text{N})_2(\text{CH}_3)][\text{X}]$ ,<sup>87</sup> are also similar: i.e., ca.  $-70$  ppm. It can be concluded that all the nitrogen atoms in complex **4** are coordinated to the rhodium metal center.  $^1\text{H}/^{13}\text{C}/^{15}\text{N}$  NMR spectra, absolute mass measurements, and elemental analyses (C, H, N, Br) indicate that complex **4** should be an octahedral ionic Rh(III)-terpyridine complex with four nitrogen atoms coordinated and one phenyl ring and one bromine atom  $\sigma$ -bonded to the rhodium center and one bromine atom serving as counteranion. However, there are two options for the binding positions of the phenyl group and the isopropylimino nitrogen atom of complex **4**. If the isopropylimino nitrogen atom is coordinated at the axial position, then the phenyl group will be in an equatorial position, and vice versa. Despite the differences between complex **4** and **22**, the coordination spheres around the rhodium metals are similar. Both contain bromides, nitrogens, and a  $\sigma$ -bonded aryl group. Therefore, the  $^1\text{H}$  NMR spectra of **4** and **22** should show similar signals and patterns in the Tpy\* aromatic region. Indeed, the  $^1\text{H}$  NMR spectra of **4** and **22** are very similar in the Tpy\*

aromatic region; i.e., the differences in charge of **4** and **22** and the deuterated solvents used ( $\text{CD}_3\text{OD}$  and  $\text{CD}_2\text{-Cl}_2$  for **4** and **22**, respectively) have little influence on the chemical shifts of e.g. the *tert*-butyl protons (H12) and most of the Tpy\* aromatic protons (3,3''; 4,4''; 5,5''; 9,9'; 14) of **4** and **22**. However, the signals belonging to H6/H6'' of **4** and **22** are shifted significantly from each other. The  $^1\text{H}(6/6'')$  NMR signal of **4** is shifted much more ( $>1$  ppm) upfield compared with the  $^1\text{H}(6/6'')$  NMR signal of **22**. A plausible explanation for this would be that the phenyl ring of complex **4** is in an equatorial position. Hence, due to the anisotropy effect, the  $^1\text{H}(6/6'')$  NMR signal of **4** is shifted upfield. For complex **22** no anisotropy effect is observed, while NOE interactions between H(6/6'') and H(14) is observed. This means that the benzene ring of complex **22** is in an axial position. Part of the shift difference of H(6/6'') in **4** and **22** may be attributed to a downfield contribution in **22** by the adjacent equatorial bromide ligand. Such a downfield shift of the H(6) proton resonance of a coordinated pyridyl ligand adjacent to an equatorial halide has been reported for Pd(II) complexes.<sup>92–94</sup> On the basis of the very similar  $^1\text{H}$  and  $^{13}\text{C}$  chemical shifts of **6–24**, it can be suggested that their Rh–carbon bond is in an axial position.

**$^{103}\text{Rh}$  NMR Spectroscopy.** Transition-metal nuclei generally offer very large changes in their chemical shift (several 100 or 1000 ppm) depending on molecular structure and, hence, good sensitivity to subtle structural perturbations, due to a large sensitivity to small changes in the ligand field.<sup>90</sup> In general, transition-metal complexes containing metal-bonded groups with more electron withdrawing and/or bulky substituents show lower shielding of the metal nuclei.<sup>90,95–99</sup> The deshielding effect correlates with the difference in ligand field energy: i.e., a lower electron density on the metal correlates with a smaller ligand field splitting and, hence, a more positive chemical shift of the metal nuclei. The steric deshielding effect correlates among other things with the metal–carbon bond length, and thus also the weakening of this bond, and hence also a more positive chemical shift of the metal nuclei with increasing M–C bond length.<sup>90</sup> However, it must be noted that the individual influences of the electronic and steric effects are difficult to separate.<sup>90</sup> Furthermore, for the transition-metal chemical shift, the ligand field (electronic and stereochemical environment) of transition-metal-containing complexes is a more dominant factor than the actual charge of the transition metal.<sup>100–104</sup>

(92) Laine, T. V.; Piironen, U.; Lappalainen, K.; Klinga, M.; Aitola, E.; Leskela, M. *J. Organomet. Chem.* **2000**, *606*, 112–124.

(93) Meneghetti, S. P.; Lutz, P. J.; Kress, J. *Organometallics* **1999**, *18*, 2734–2737.

(94) Rülke, R. E.; Delis, J. G. P.; Groot, A. M.; Elsevier, C. J.; Van Leeuwen, P. W. N. M.; Vrieze, K.; Goubitz, K.; Schenk, H. J. *Organomet. Chem.* **1996**, *508*, 109–120.

(95) Von Philipsborn, W. *Pure Appl. Chem.* **1986**, *58*, 513.

(96) Maurer, E.; Rieker, S.; Schollbach, M.; Schwenk, A.; Egolf, T.; Von Philipsborn, W. *Helv. Chim. Acta* **1982**, *65*, 26.

(97) Täschler, K. University of Zürich, Zürich, 1990.

(98) Tavagnacco, C.; Balducci, G.; Costa, G.; Täschler, K.; Von Philipsborn, W. *Helv. Chim. Acta* **1990**, *73*, 1469.

(99) Asaro, F.; Costa, G.; Dreos, R.; Pellizer, G.; Von Philipsborn, W. *J. Organomet. Chem.* **1996**, *513*, 193.

(100) Ramsey, N. F. *Phys. Rev.* **1950**, *77*, 567.

(101) Ramsey, N. F. *Phys. Rev.* **1950**, *78*, 699.

(102) Ramsey, N. F. *Phys. Rev.* **1951**, *83*, 540.

(103) Ramsey, N. F. *Phys. Rev.* **1952**, *86*, 243.

(104) Griffith, J. S.; Orgel, L. E. *Trans. Faraday Soc.* **1957**, *53*, 601.

This is clearly evidenced for complex **4**. Although complex **4** contains a cationic Rh(III) metal, suggesting an electron-poor metal center, complex **4** has the lowest  $\delta(^{103}\text{Rh})$  value of the Rh(III)-terpyridine complexes studied. This can be explained by the fact that complex **4** contains an additional N atom instead of a bromide, which accounts for the somewhat lower  $\delta(^{103}\text{Rh})$  value compared to e.g. **6** or **14**.

The Rh metal nucleus has a great sensitivity to (small) changes in its coordination environment. This has been amply demonstrated in previous studies,<sup>105–108</sup> which is also observed by comparing the  $\delta(^{103}\text{Rh})$  values for the octahedral Rh(III) complexes **4–7**, **9**, **13–17**, **22**, and  $[(R^3)\text{Rh}^{\text{III}}(\text{Cl})_2(2,6-(\text{C}(\text{R}^1)=\text{NR}^2)_2\text{C}_5\text{H}_3\text{N})]$ .<sup>74</sup> The  $\delta(^{103}\text{Rh})$  signal for  $[(R^3)\text{Rh}^{\text{III}}(\text{Cl})_2(2,6-(\text{C}(\text{R}^1)=\text{NR}^2)_2\text{C}_5\text{H}_3\text{N})]$  is generally more positive than for complexes **4–7**, **9**, **13–17**, and **22**. This is most probably due to the fact that chloride is lower in the spectrochemical series compared to bromide ( $R^3$ , Table 8). Furthermore, the imine nitrogens in  $[(R^3)\text{Rh}^{\text{III}}(\text{Cl})_2(2,6-(\text{C}(\text{R}^1)=\text{NR}^2)_2\text{C}_5\text{H}_3\text{N})]$  must be regarded as higher in the spectrochemical series as compared with the pyridine nitrogens in Rh(III)-terpyridine complexes, since the former are better  $\pi$ -acceptors.

Apart from relatively small mutual differences, complexes **4–7**, **9**, **13–17**, **22**, and  $[(R^3)\text{Rh}^{\text{III}}(\text{Cl})_2(2,6-(\text{C}(\text{R}^1)=\text{NR}^2)_2\text{C}_5\text{H}_3\text{N})]$  show similar trends in chemical shifts within their respective series in relation to deshielding of the nuclei. As has been shown before and was discussed above, the nuclear deshielding correlates qualitatively at least with the relative ligand field energy: i.e., a lower electron density on the metal correlates with a smaller ligand field splitting and, hence, a more positive chemical shift of the metal nuclei.

For compounds **A–G** (Table 8), the following qualitative assessment can be made. Compound **G** contains a halide directly coordinated to Rh and, hence, a much higher chemical shift compared to the strong-field  $\text{CH}_2\text{X}$  moiety of the other compounds in this subseries. The

(105) Mann, B. E. *Transition Metal Nuclear Magnetic Resonance*; Elsevier: Amsterdam, 1991.

(106) Bonnaire, R.; Davoust, D.; Platzer, N. *Org. Magn. Reson.* **1984**, *22*, 80.

(107) Ernsting, J. M.; Elsevier, C. J.; De Lange, W. G. J. *Chem. Commun.* **1989**, 585.

(108) Elsevier, C. J.; Kowall, B.; Kragten, H. *Inorg. Chem.* **1995**, *34*, 4836–4839.

shift of **C** relative to **A** and **B** is explained by the fact that the coordination angles within the complexes are far from optimum especially in **C**;<sup>74</sup> hence, the ligand field splitting is less for this complex, resulting in a higher chemical shift. Other differences are rather small and cannot be explained even qualitatively.

The complexes  $[(R^3)\text{Rh}^{\text{III}}(\text{Cl})_2(2,6-(\text{C}(\text{R}^1)=\text{NR}^2)_2\text{C}_5\text{H}_3\text{N})]$  and **4–7**, **9**, **13–17**, and **22** show similar trends. This is best evidenced by comparing the  $\delta(^{103}\text{Rh})$  value of complex **5** and those of complexes **6**, **7**, **9**, **13–17**, and **22**. Like complex **G**, complex **5** contains three Rh–X  $\sigma$ -bonds ( $X = \text{Br}$ ) and has by far the most positive  $\delta(^{103}\text{Rh})$  within the subseries, since **4**, **6**, **7**, **9**, **13–17**, and **22** contain only two Rh–Br  $\sigma$ -bonds. Furthermore, complexes **14–16** and **22** have more positive  $\delta(^{103}\text{Rh})$  values than complexes **6**, **7**, **9**, and **13**. Apparently, vinyl, allyl, and phenyl groups induce a lower ligand field than alkyl groups.

**Monitoring the Formation of Complex 13 with UV/Vis Spectrometry: Mechanistic Aspects.** When the formation of complex **13** from complex **2** and 1-bromodecane is monitored, in absence of *o*-cresol, isosbestic points in the electronic absorption spectra are clearly observable (Figure 3). However, the involvement of possible formed intermediates, during the synthesis of complex **13**, cannot be excluded. Radicals as intermediates can be excluded, since monitoring the oxidative addition reaction in the presence of *o*-cresol gave electronic absorption spectra similar to those without *o*-cresol.

TD-DFT calculations<sup>89</sup> have shown that the HOMO of complex **2** is entirely located on the  $d_{z^2}$  orbital of the Rh metal. This doubly occupied  $d_{z^2}$  HOMO then nucleophilically attacks the bromine-bearing carbon bond and forms the new Rh–carbon bond concurrently with the breaking of the carbon–bromine bond: i.e., for complexes **6–24** the new Rh–carbon bond is in an axial position with respect to the equatorial Rh–Tpy\* plane. Only, as evidenced by NMR, in complexes **3** and **4** is the Rh–carbon bond in an equatorial position.

However, on the basis of the results, it is not possible to unequivocally propose a mechanism of the overall oxidative addition of the carbon–halogen bonds to Rh(I)-terpyridine complexes.

OM0305418